High efficiency of two solar cells CIGS/CIS stacked mechanically

Y. Mir[a], M. Khalis[a], A. Nafidi[b] and M. Zazoui*[a]

[a] *Laboratory of Condensed Matter, Faculty of Sciences and Techniques, University of Hassan II Mohammedia, Casablanca, Avenue Hassan II, BP 146, 28800 Mohammedia, Morocco*

[b]*Laboratory of Condensed Matter Physics and Nanomaterials for Renewable Energy, Department of Physics, Faculty of Sciences, BP 8106 Hay Dakhla;University Ibn Zohr, 80000 Agadir, Morocco.*

**corresponding author : zazouimimoun@yahoo.fr*

Abstract: In our work, we have simulated and optimized solar cells based on the mechanically stacked system using the Analysis of Microelectronic and Photonic Structures (AMPS-1D) simulator in respect to overall performance. The structures of solar cells are based on the top cell Copper- Indium-Gallium- diselenide, $CuIn_{1-x}Ga_xSe_2$, referred to as CIGS, and the bottom cell Copper- Indium-Gallium, CIS. We have simulated each cell individually and extrapolated their optimal parameters (thickness, concentration of absorber). In the case of tandem, we calculated the efficiency of each cell optimized by separation of the solar spectrum in bands where the cell is sensible for the absorption. The current-matching limitation imposed by series connection reduces efficiency relative to independently-connected cells.

Key-Words: AMPS-1D, thin-film, single junction, tandem, Cu (In, Ga) Se2 (CIGS), CIS, conversion efficiency.

I. Introduction

In practice, efficient spectral splitting is hard to achieve. A more practical strategy is to stack different band gap junctions in optical series [1-5], and allow the wider band gap materials at the top to filter out most of the high energy photons, while less energetic photons pass through to smaller band gap materials below. Greatest power is extracted if the output from the different junctions can be independently optimised.

Thin-film solar cells based on $CuInSe_2$ (CIS) absorber with a band gap of E_g = 1.04 eV and also based on $CuIn_{1-x}Ga_xSe_2$ (CIGS) alloy absorbers with a band-gap range of Eg = 1.0 – 1.67 eV are investigated in this work. $CuInSe_2$-based solar cells have shown long-term stability and the highest conversion efficiencies among all thin-film solar cells, reaching 20 % [6].

The value of the CIGS band gap correlates with white-light performance of these cells. It has been observed earlier by others [7-11] and also in this work, that CdS/CIGS cells with Eg(CIGS) above ~ 1.15 eV are limited in their open-circuit voltage V_{OC}. Our results show that the addition of the CIS cell in series with the CIGS cell, increases open circuit V_{OC} and consequently the efficiency.

The use of thin film technology for the fabrication of solar cells has gradually been increasing due to lower production costs and greater efficiency, compared to other kinds of solar cells [12]. The conversion efficiency of a solar cell can be increased significantly with the improvement of the properties of the materials and subsequently the designs and structures of the cell. Copper- Indium-Gallium- diselenide, CIGS alloy has become one of the important semiconductor materials for solar cells due to its low cost and the easy fabrication process. Hetero-junction solar cells, where two different materials with different band-gaps form a junction, are of great interest to many researchers.

Multi-junction compound semiconductor solar cells have consistently demonstrated their performance as the highest efficiency cells, thanks to their ability to absorb a greater proportion of the solar spectrum more effectively. High efficiency triple junction solar cells have recently been produced with efficiencies of approximately 39% [13]. To achieve the highest efficiencies, the optoelectronic properties of the materials used in multi-junction solar cells must be optimized to absorb and convert efficiently as much of the solar flux as possible. One of the primary difficulties with these devices is evaluating new design approaches.

In this study, we have designed two types of solar cell models with single and double junctions having the structure of CIGS and CIGS/CIS respectively.

In practice, the single junction cell usually can give higher efficiency due to the leakage of maximum energy utilization of solar energy. For that, we have designed the multi-junction solar cells, such as double junctions, based on the spectral splitting principle so that the maximum energy can be absorbed. Moreover, the light induced degradation, i.e. higher instability in single junction cells, leads us to design stacked structures for capturing the solar spectrum efficiently, then it can achieve the maximum conversion efficiency [13, 14].

When alloying the $CuInSe_2$ (CIS) with Ga to form CIGS thin films, the wider band-gap energy of the CIGS absorber layer can potentially better match the solar

spectrum, as well as increase the V_{OC} of the fabricated cells, at the expense of a reduction in the value of the short-circuit current density (J_{SC}). Introducing a spatial variation of the Ga content within the CIGS layer, the band-gap profile can be optimized to increase the photon absorption and carrier diffusion. Furthermore, the Ga profile can be adjusted to optimize the CIGS absorber band gap profile, and hence improve the V_{OC} and J_{SC} values. Thus, band-gap engineering, geared to controlling the spatial distribution of the Ga content in the absorber layer, can lead to the enhancement of the overall performance of CIGS cells.

In this paper, device modelling and numerical simulations of CIGS cells are conducted to analyze the impacts of various band-gaps for the CIGS layers on the efficiencies of the cells. Such modelling works will provide insight into which structures may be desirable for tandem cells. The investigation focuses on the study of the effect on performance caused by various band-gap profiles on the current matching limitation imposed by series connection.

II. Cell Structure and Material Parameters

The schematic energy-band diagram under equilibrium condition for a typical ZnO/CdS/CIGS solar cell with a uniform band-gap profile is illustrated in Figure 1. The CIGS cell structure considered in this study consists of the following material layers: n-ZnO, n-CdS, high-recombination interface, p-CIGS absorber. The computer simulation tool AMPS-1D (Analysis of Microelectronic and Photonic Structures, developed by S. Fonash and colleagues at Pennsylvania State University) [15] was employed by specifying as input values the semiconductor parameters in each layer of the cell structure (see table 1). The division of the layers for the cell structure is limited to the simplified device structure described above because of the limited knowledge available on the semiconductor parameters in each layer and uncertainties in the interface and junction properties arising from possible inter-diffusion and reaction during the cell processing.

The band gap of the CIGS absorber is engineered through the addition of a Ga profile. The anticipated changes in the physical properties of the CIS films with the addition of Ga include an increase in band gap, which mainly shifts the position of the conduction-band minimum [16], as well as changes in the hole concentration [17], bulk defect densities [18], absorption coefficients, and electron affinities. The room temperature mobility was found to be 300K and remains nearly constant while varying the Ga content over a wide range [17].

Table 1: Semiconductor properties of the intrinsic ZnO, CdS, and CIGS layers as the input parameters for the simulations Parameters for the base case

	Front Surface (x=0µm)	Back Surface (x=2 µm)
$\Phi_{b0/L}=E_C - E_F$	0.0 eV	0.8 eV
Surface recombination electrons	10^7 cm/S	10^7 cm/S
Surface recombination holes	10^7 cm/S	10^7 cm/S
Reflectivity	0.05	0.8

	ZnO	CdS	CIGS
Width	50 nm	50 nm	2000 nm
Dielectric constant	9.0	10	13.6
Electron mobility	100 cm^2/Vs	100 cm^2/Vs	200 cm^2/Vs
Hole mobility	25 cm^2/Vs	25 cm^2/Vs	5 cm^2/Vs
Carrier density	$N_D= 10^{18}$ cm^{-3}	$N_D= 10^{17}$ cm^{-3}	$N_A= 2\ 10^{16}$ cm^{-3}
Band-gap	3.3 eV	2.4 eV	1.15 eV
Effective dens. N_C	2.2×10^{18} cm^{-3}	2.2×10^{18} cm^{-3}	2.2×10^{18} cm^{-3}
Effective dens. N_V	1.78×10^{19} cm^{-3}	1.78×10^{19} cm^{-3}	1.78×10^{19} cm^{-3}
Electron affinity	4.0 eV	3.8 eV	4.1 eV
Gaussian defects	ZnO	CdS	CIGS
Defect density	$N_{DG}=10^{17}$ cm^{-3}	$N_{AG}=10^{18}$cm^{-3}	$N_{DG}=10^{14}$ cm^{-3}
Peak energy	midgap	midgap	midgap
Standard deviation	0.1 eV	0.1 eV	0.1 eV
Cross-section electronique.	1.2×10^{-12} cm^2	10^{-17} cm^2	5.3×10^{-13} cm^2
Cross-section holes	10^{-17} cm^2	9.8×10^{-13} cm^2	10^{-18} cm^2

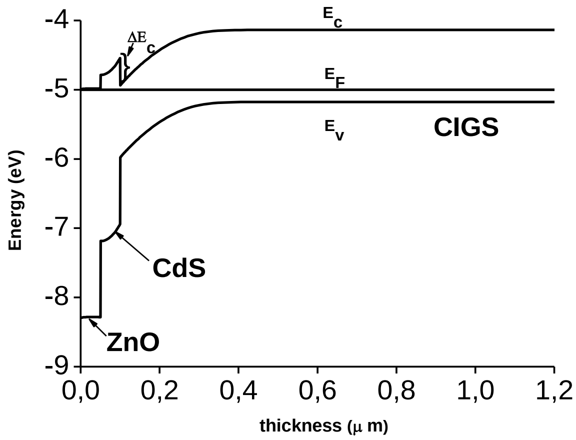

Figure 1. A simulated band diagram of, a typical CIGS (1.15 eV) solar cell

First, a simulation study of band-gap 1.15 eV for a CIGS cell is carried out to establish a baseline for choosing the thickness and concentration of absorber. The simulation results are shown in figure 2. Second, a simulation study of cell efficiency dependence on the band gap of CIGS absorbers is carried out.

Third, a simulation study was conducted to evaluate the effect of band-gap profile of the CIGS absorber on the performance of the tandem cells.

III. Result and discussion

In the first part, the calculated impact of the CIGS hole density on devices with different thicknesses is shown in fig. 2. Increasing hole density decreases the space-charge region width, resulting in a trade between voltage and current:

The voltage dependence on doping for devices thicker than 1μm is linear on a semi- logarithmic scale for a doping superior to $10^{15}cm^{-3}$. For submicron devices, the voltage follows the same behaviour when the thickness of the device is larger than the SCR width. When the device is fully depleted however, the voltage benefit of higher doping saturates.

Current decrease is due to a shorter high- field region with higher hole densities. It shows similar trends for different CIGS thicknesses. For thinner devices, however, the current losses at higher carrier densities become more pronounced. For the thinnest device analyzed, d = 250 μm, once the hole density is high enough to lower the depletion region width below the absorber thickness, the current decrease is more abrupt compared to other devices. FF is also affected for very thin absorbers and very high hole densities.

For thick devices (d ≥ 1 μm), the voltage gain resulted from increased absorber doping is generally higher than the current loss, and therefore the hole density increase can improve the efficiency. For submicron devices, however, the typical voltage gain is comparable to the current loss, and for ultra-thin devices and high hole densities, the collection losses are high enough to decrease the overall performance. Once the device is fully depleted, the performance is independent of the carrier density (horizontal parts in all parameters at low carrier densities).

Therefore, the $Cu(In_{1-x},Ga_x)Se_2$ cell with composition x ≈ 0.3 and Eg ≈ 1.15 eV [19-21] has a high efficiency at thickness 2μm and a concentration $N_a=2.10^{16}cm^{-3}$.

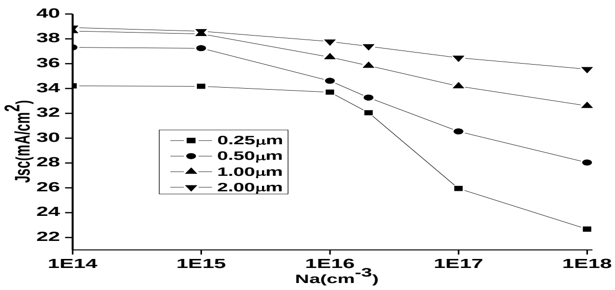

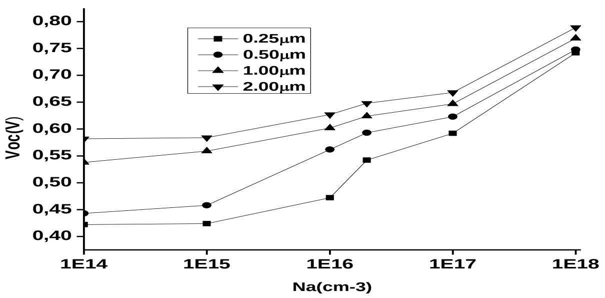

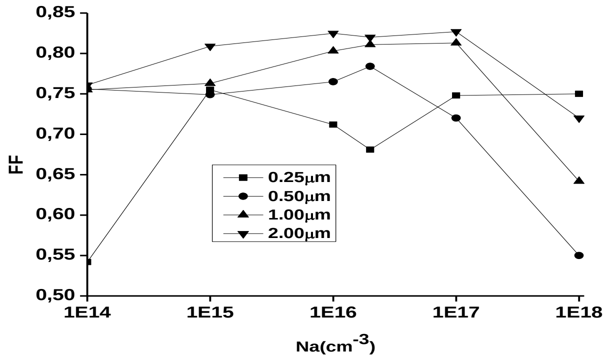

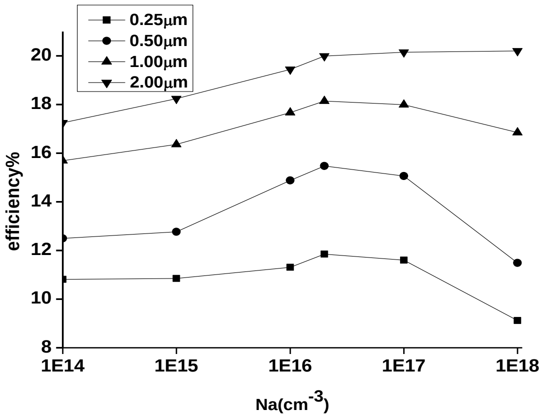

Figure 2. Calculated impact of CIGS hole density on V_{OC}, J_{SC}, FF and efficiency for 2 μm, 1 μm, 0.50 μm and 0.25 μm devices.

In the second part, we have fixed the doping of the absorber at N_a~$2.10^{16}cm^{-3}$ and the thickness at d~2 μm, and can see the impacts of various band-gaps for the CIGS layers on the efficiencies of the cells; figure 3 shows that:

For the band gap of CIGS absorbers (1.1 to 1.4 eV), the efficiency (η) increases until (19.5-19.6%) thanks to the V_{OC} linearly increase and the current lightly decreases. But from 1.4 eV onward the efficiency (η) decreases, and there is a clear reduction of J_{SC} because most of photons are not absorbed.

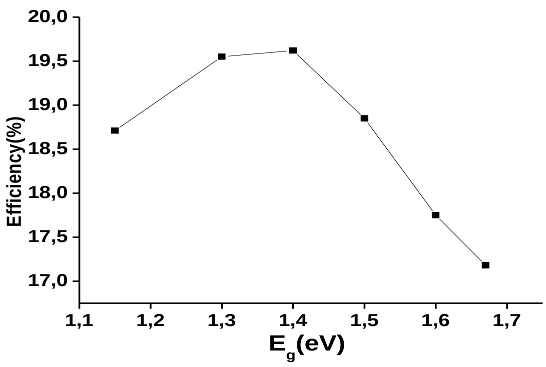

Figure 3. Conversion efficiency with variable band gap.

In the third part, we study the simulation of tandem cells by varying the gap of the top CIGS cell in order to deduce the cell that gives the best efficiency with the CIS bottom. The current-bias curves are calculated for each individual cell using the incident solar flux that is filtered by the absorption of the cells above (see figure 3).

Then current matching is enforced by $J_{SC,min}$ = min ($J_{SC,CIS}$; $J_{SC,CIGS}$) , the voltage $V(J_{SC,\ min}) = \sum V(J_{SC,\ min})$ and the efficiency $\eta = J_{SC,min}(V_{CIS} + V_{CIGS}) / P_{in}$, where P_{in} is the incident light power on the cell. It is commonly taken to be 100 mW/cm^2 for standard solar illumination. This illumination is referred to as AM 1.5 illumination, and it is equivalent to sunlight passing through 1.5 times the air mass of vertical illumination.

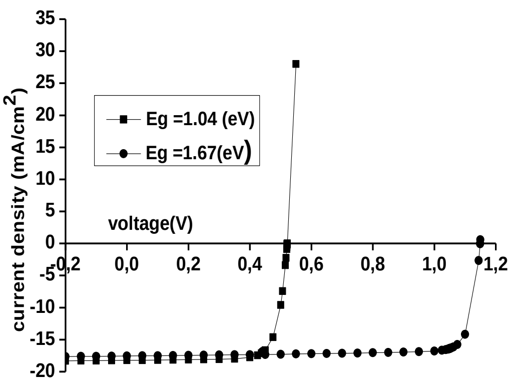

Figure 4. Simulated current -voltage curves solar cells tandem with top Eg(CIGS) = 1.6 eV and bottom Eg(CIS)=1.04 eV

The simulation results are shown in figure 4, where the resulting performance parameters of V_{OC}, J_{SC}, and efficiency (η) are shown as a function of the band gap Eg(CIGS) . For top cell CIGS, the value of Voc in figure 4 (a) increases with increasing band-gap , improving from ~ 650 to ~ 1000 mV, while the value of J_{SC} in Figure 4 (b) decreases from ~ 37.77 to ~ 18.20 mA/cm^2.

For bottom cell CIS, the value of Voc in figure 3 (a) increases slightly with an increasing band-gap , improving from ~ 450 to ~ 490 mV, while the value of Jsc in figure 3 (b) increases from ~ 4,016 to ~ 18.20 mA/cm^2.

The value of η in Figure 3 (c) increases from ~ 4.6% at a value of ~ 1.15 eV to a maximum value of ~ 27.87% at a value of ~ 1.50 eV.

Conclusion

Device modelling and numerical simulations of the CIGS solar cells with consideration of different junction formation and various junction parameters have been carried out using the AMPS-1D program. A detailed analysis of the effects of the band gap of the absorbers has been presented. Therefore, the open-circuit voltage and fill factor of CIGS solar cells are improved. Thus, the efficiency of the devices is enhanced.

Reduced photon flux absorbed in the wide-gap buffer in top cell CIGS may result in reduction of the current in the bottom cell CIS, hence $CuInSe_2$ is a good candidate for the absorber material in the bottom cells of thin-film tandem solar cells.

The tandem realized by stacking two cells mechanically: shown previously, has the best features. In fact, it uses a wider spectral range and has an energy conversion efficiency of ~27.99% and open-circuit-voltage of ~1.5 V under the AM1.5 spectrum at room temperature and without concentration.

References:

[1] Wanlass, M.W., Albin, D.S., 2004. AIP Conf. Proc. 738, 462.

[2] Trivich, D., Flinn, P. A., 1955. Maximum efficiency of solar energy conversion by quantum processes, Solar Energy Research, Eds. Madison, WI: Univ. of Wisconsin Press 143.

[3] Jackson, E.D., 1955. “Areas for improvement of the semiconductor solar energy converter,” in Trans. Intern. Conf. Use of Solar Energy-The Scientific Basis, vol. 5, 122.

[4] Khalis, M., Mir,Y., Zazoui, M., 2010. International Scientific Journal for Alternative Energy and Ecology. ,No. 11, 60.

[5] Nakada ,T., Hirabayashi ,Y. , Tokado ,T. and Ohmori, D., 2004. Solar Energy, vol. 77, s739.

[6] Singh Udai, P. and Patra Surya , P., 2010. International Journal of Photoenergy, vol. 2010

[7] Luque, A. and S. Hegeds, 2003. Eds., Handbook of Photovoltaic Science & Engineering, John Wiley & Sons, New York, NY, USA.

[8] Markvantand , T., Castarier, 2003. Eds., Practical handbook of Photovoltaics: Fundamentals and Applications,Elsevier, Amsterdam, The Netherlands.

[9] Archer, M. D., and Hill, R., 2001. Eds., Clean Electricity from Photovoltaics, vol. 1, chapter 7 of Series on Photoconversion of Solar Energy .

[10] Romeo, A., Terheggen , M., Abou-Ras, D. et al., 2004. “Development of thin-film Cu(In,Ga)Se2 and CdTe solar cells,” Progress in Photovoltaics: Research and Applications,vol.12 93.

[11] Kemell, M., Ritala, M., and Leskel¨, M. , 2005. “Thin film deposition methods for CuInSe2 solar cells,” Critical Reviews in Solid State and Materials Sciences, vol. 30, 1.

[12] Gregg, A., Blieden, R., Chang, A., and Ng, H., 2005. Performance Analysis of Large Scale, Amorphous Silicon Photovoltaic Power Systems, Photovoltaic Specilist Conference and Exhibition, Florida, USA, January, 3.

[13] King, R., et al., 2005. Pathways to 40%-efficient concentrator photovoltaics. Proceedings of the 20th European Photovoltaic Solar Energy Conference.

[14] Li, L., Chae, Y. K., Sheng, S., Won, T. K. , Kadam, A., Chen, J. , Choi, S. Y. , and White, J. M., 2007. “a Si:H single junction and a-Si:H/C-Si:H tandem solar

cells fabrication using large area (5.7 m^2) PECVD systems". Technical Digest of the international, Fukuoka, Japan, PVSEC-17

[15] Zhu, H., Kalkan, A.K., Hou, J., Fonash, S.J., 1999. Application of AMPS-1D for solar cell simulation. AIP Conf. Proceedings; 462, 309.

[16] Wei, S.H., Zunger, A., 1995. Band offsets and optical bowings of chalcopyrites and Zn-based II-VI alloys. J. Appl. Phys, 78, 3846.

[17] Schroeder, D.J. , Hernandez, J.L., Rockett, A.A. , 1999. Point defects and hole transport in epitaxial CuIn1-xGaxSe2. 11th Int. Conf. on Ternary and Multinary Compounds 749.

[18] Hanna, G., Jasenek, A., Rau, U., Schock, H.W., 2001. Influence of the Ga-content on the bulk defect densities of Cu(In,Ga)Se2.Thin Solid Films, 387, 71.

235.

[19] FonAsh, S.V., Arch, J., Cuiffi, J., Hou, J., Howland, W., McElheny, P. , Moquin, A., Rogossky, M., Rubinelli, F. , Tran, T., and Zhu, H., 1997. A manual for AMPS-1D for Windows 95/NT; A one-dimensional device simulation program for the analysis of microelectronic and photonic structures. Pennsylvania State University, USA

[20] Repins, I., Contreras, M., et al., 2008. Presented at the 33rd IEEE Photovoltaic Specialists Conference San Diego, California, Conference Paper NREL/CP-520-42539

[21] Repins, I., Contreras, M. A. , Egaas, B. et al., 2008. "19.9%-efficient ZnO/CdS/CuInGaSe2 solar cell with 81.2% fill factor," Progress in Photovoltaics: Research and Applications, vol. 16

